CURRENT BIOCHEMISTRY

Article

Virtual Screening of Flavonoids Similar to Isoliquiritigenin as Inhibitors of FMS-like Tyrosine Kinase-3 (FLT3)

Wildan Aulia Noorsy [1], Popi Asri Kurniatin [1,*] and Ukhradiya Magharaniq Safira Purwanto [1]

[1] Department of Biochemistry, IPB University, Bogor, 16680, Indonesia
* Correspondence: popi_asri@apps.ipb.ac.id

Abstract: *Acute myeloid leukemia is a type of leukemia caused by the disruption of the maturity of the hematopoiesis process at the myeloid lineage. The cause is a mutation in FMS-like tyrosine kinase 3 (FLT3) that triggers unregulated proliferation and differentiation signaling, so it can be used as a target receptor in its treatment. This study aims to find flavonoid compounds as potential compounds for FLT3 inhibitors. The method in this study uses a similarity search to isoliquiritigenin to search for flavonoids and then uses virtual screening techniques and molecular docking of FLT3 as well as predictions of its bioavailability and toxicity properties. This study resulted in 60 ligands from similarity search results. After conducting virtual screening, molecular docking, and prediction of bioavailability, and toxicity, 13 test ligands were found that have the potential to be drug candidates. This research concludes that sophoradin has a bond-free energy (ΔG) of -9,697 kcal/mol which is the ligand as the strongest bonding in this research. The results are potential for further research as FLT3 inhibitors as candidates for the treatment of acute myeloid leukemia.*

Keywords: flavonoid, FLT3, isoliquiritigenin, molecular docking, similarity search

Abstrak: Leukemia myeloid akut merupakan jenis leukimia yang disebabkan karena terjadinya hambatan maturitas proses hematopoiesis pada garis keturunan myeloid. Penyebabnya adalah terjadinya mutasi pada FLT3 yang memicu persinyalan proliferasi dan diferensiasi yang tidak teregulasi sehingga dapat dijadikan reseptor target dalam pengobatannya. Penelitian ini bertujuan mencari senyawa flavonoid yang berpotensi sebagai inhibitor FLT3. Metode dalam penelitian ini menggunakan *similarity search* terhadap *isoliquiritigenin* untuk mencari flavonoid lalu digunakan teknik penapisan virtual dan simulasi penambatan molekuler terhadap FLT3 serta prediksi sifat bioavailabilitas dan toksisitasnya. Hasil penelitian ini menghasilkan 60 ligan uji hasil *similarity search*. Setelah penapisan virtual, penambatan molekuler, dan prediksi bioavailabilitas, dan toksisitas dihasilkan 13 ligan uji yang berpotensi dijadikan kandidat obat. Simpulan penelitian ini menunjukan bahwa *sophoradin* memiliki energi bebas ikatan (ΔG) -9,697 kkal/mol dan merupakan ligan dengan potensi pengikatan terkuat dalam inhibisi FLT3. Hasil penelitian berpotensi digunakan dalam penelitian lebih lanjut sebagai inhibitor FLT3 sebagai kandidat pengobatan leukemia myeloid akut.

Kata kunci: flavonoid, FLT3, *isoliquiritigenin*, penambatan molekuler, *similarity search*

Citation: Noorsy WA, Kurniatin PA, Purwanto UMS. 2026. Virtual screening of flavonoids similar to isoliquiritigenin as inhibitors of FMS-like Tyrosine Kinase-3 (FLT3). *Current Biochemistry.* 13(2): 1-10.

Received: August 6th, 2026
Revised: August 10th, 2026
Accepted: August 10th, 2026
Published: August 12nd, 2026

Copyright: © 2026 by the authors. Submitted for possible open access publication under the terms and conditions of the Creative Commons Attribution-ShareAlike 4.0 International License (http://creativecommons.org/licenses/by-sa/4.0/).

pISSN: 2355-7877
eISSN: 2355-7931

1. Introduction

Hematopoiesis is the essential biological process of blood cell formation from hematopoietic stem cells (HSCs) initiated during embryonic development and maintained throughout adulthood to sustain the circulatory system (Jagannathan-Bogdan and Zon, 2013). HSCs give rise to both myeloid lineages, including macrophages, monocytes, and erythrocytes, and lymphoid lineages such as T-cells and B-cells (Birbrair and Frenette, 2016). To maintain physiological homeostasis, the human body must produce approximately 500 billion new blood cells daily (Nombela-Arrieta and Manz, 2017). The regenerative capacity and multipotent differentiation of hematopoietic stem and progenitor cells (HSPCs) require precise regulation, as genetic dysregulation within these cells can lead to diverse hematological malignancies. Specific leukemogenic mutations disrupt inhibitory pathways of cell differentiation, thereby inducing uncontrolled proliferation and enhanced cell survival (Basilico and Gottgens, 2017).

A critical driver in this pathological process is the mutation of the FMS-like tyrosine kinase 3 (FLT3) gene located on chromosome 13q12. Identified in 30% to 35% of patients with acute myeloid leukemia (AML), FLT3 mutations represent one of the most frequent genetic alterations in the disease (Kantarjian *et al.*, 2021). FLT3 functions as a class III receptor tyrosine kinase (RTK) and is expressed in hematopoietic progenitor cells where it governs key signaling cascades (Kawase *et al.,* 2019). Under physiological conditions, the receptor remains inhibited until ligand binding triggers homodimerization and transphosphorylation. This activation stimulates downstream pathways, including PI3K, AKT, and STAT5, which are vital for cell survival and proliferation (Sutamtewagul and Vigil, 2018). However, mutations such as internal tandem duplication (ITD) and point mutations in the tyrosine kinase domain (TKD) lead to constitutive signaling activation independent of ligand presence (Papaemmanuil *et al.*, 2016).

The clinical burden of AML remains significant, with a global incidence of approximately one million cases and a five-year survival rate that remains poorly optimized despite therapeutic advancements (Egbuna *et al.*, 2021; Vos *et al.*, 2016). While synthetic inhibitors like sorafenib and gilteritinib demonstrate efficacy, the development of drug resistance and adverse side effects necessitates the exploration of natural product-based inhibitors (Kawase *et al.*, 2019). Flavonoids, a group of bioactive polyphenolic secondary metabolites, have emerged as promising candidates due to their potent anti-inflammatory and anticancer properties (Kopustinskiene *et al.*, 2020). Specifically, the flavonoid isoliquiritigenin (ISL) has demonstrated significant FLT3 inhibition in both in vitro and in vivo models, suggesting its potential as a therapeutic agent with reduced toxicity (Wang *et al.*, 2021; Cao *et al.*, 2019). Beyond its documented bioactivity, ISL was chosen as the structural template for this study because its chalcone scaffold, a reactive benzene ring bearing hydroxyl and carbonyl substituents, provides a chemically tractable starting point for identifying structurally related flavonoids with comparable or improved FLT3-binding potential. While ISL itself has established FLT3-inhibitory activity, its close structural analogues remain largely unexplored as potential inhibitors, which directly motivates the similarity-search strategy adopted here.

Modern drug discovery increasingly relies on in silico methods to enhance success rates while minimizing laboratory costs and timeframes (Egbuna *et al.*, 2021). Utilizing similarity searches within the PubChem database allows for the identification of compounds with analogous 2D and 3D structures, facilitating the discovery of molecules with similar bioactivity (Kim *et al.*, 2016). Consequently, this study aims to identify flavonoid compounds based on structural similarity to isoliquiritigenin that exhibit FLT3 inhibitory activity. This research serves as a computational screening step to discover novel candidates for the treatment of acute myeloid leukemia.

2. Materials and Methods

2.1. Materials

Computational simulations were performed on a Windows 10 (64-bit) platform equipped with an Intel® Celeron® CPU 4205U @ 1.80 GHz and 4 GB RAM. Molecular docking and energy minimizations were conducted using YASARA Structure (licensed by the Department of Biochemistry). Supporting software included Discovery Studio 2017, LigPlot+ 4.3.5, and PyMOL for the visualization of ligand-receptor interactions.

The 3D crystal structure of the human FMS-like tyrosine kinase (FLT3) receptor was retrieved from the RCSB Protein Data Bank (PDB ID: 6JQR). Ligand structures, including the control compounds (isoliquiritigenin and the clinical inhibitor gilteritinib), were obtained from the PubChem database.

2.2 Ligand Library and Receptor Preparation (Egbuna *et al.* 2021)

The 3D crystal structure of human FMS-like tyrosine kinase 3 (FLT3) was retrieved from the RCSB Protein Data Bank (PDB ID: 6JQR). Receptor preparation involved removing water molecules and non-essential residues, extracting the co-crystallized ligand, and adding polar hydrogens.

A ligand library was constructed via similarity searches of isoliquiritigenin on PubChem. The 2D search used an 881-bit PubChem substructure fingerprint with a Tanimoto coefficient threshold of ≥ 0.9, while the 3D search applied a Gaussian-shape overlay method evaluating Shape-Tanimoto and Color-Tanimoto scores (Kim et al., 2016; Bolton et al., 2011). Based on 2D and 3D relevance, 60 phenolic derivatives were selected. Control ligands included isoliquiritigenin, on the basis of its previously reported FLT3-inhibitory activity (Wang et al., 2021; Cao et al., 2019), and the known FLT3 inhibitor gilteritinib, a clinically approved FLT3 inhibitor (Kawase et al., 2019; Sutamtewagul and Vigil, 2018). All 3D structures (*.sdf) were optimized through energy minimization in YASARA and converted to *.pdb format.

2.3 Docking Method Validation (Land and Humble 2018)

To ensure the reliability of the docking parameters, the co-crystallized ligand was re-docked into the FLT3 active site. The grid box size was optimized by evaluating a range from 1.0 to 5.0 Å with 0.5 Å intervals. The protocol was considered validated if the Root Mean Square Deviation (RMSD) between the predicted pose and the experimental crystal structure was < 2.0 Å.

2.4 Virtual Screening and Molecular Docking (Dallakyan and Olson 2015)

Virtual screening of the 60 candidate ligands was performed using the validated grid box coordinates. Initial screening utilized the dock_runscreening.mcr macro (100 runs per ligand). Top-performing candidates, identified by superior binding energy compared to controls, proceeded to intensive molecular docking. This secondary stage employed the dock_runlocal.mcr macro with 999 iterations to ensure convergence and local search exhaustion (Ochieng *et al.*, 2017).

2.5 Interaction Analysis and ADMET Prediction (Choudhary *et al.,* 2020)

Ligand-receptor complexes were analyzed for Gibbs free energy (ΔG), inhibition constants (Ki), and binding affinity. The 2D and 3D interaction maps were generated to identify hydrogen bonds and hydrophobic contacts.

The pharmacokinetic profile of the lead compounds was evaluated through bioavailability and toxicity prediction. Bioavailability was predicted by assessing Lipinski's Rule of Five (MW < 500 Da, LogP < 5, H-bond donors < 5, and H-bond acceptors < 10) via the TargetNet server, while toxicological risks were evaluated using the admetSAR platform (Daina *et al.*, 2017).

3. Results

3.1. Ligand Similarity Search and Selection

The 2D and 3D similarity searches based on the isoliquiritigenin scaffold yielded 2,385 and 775 compounds, respectively. Based on structural relevance and classification within the flavonoid group, 60 candidate ligands were selected, 30 from 2D and 30 from 3D searches (Table 1). Analysis revealed a structural overlap between the two search methods, with seven ligands from the 2D set present in the 3D results, and six ligands from the 3D set identified in the 2D results.

Table 1. Candidate ligand identified through 2D and 3D similarity searches.

No	2D Similarity Search Ligands	No	3d Similarity Search Ligands
1	Phloretin	1	Pinocembrin chalcone
2	Eriodictyol chalcone	2	Helichrysetin
3	2',4'-Dihydroxychalcone	3	Nubigenol
4	2'-Methylisoliquiritigenin	4	Robtein
5	Okanin	5	Licodione
6	2',4',6'-Trihydroxydihydrochalcone	6	Naringenin chalcone
7	Neosakuranetin	7	2'-aminochalcone
8	Paratocarpin E	8	4,2'-dihydroxydihydrochalcone

No	2D Similarity Search Ligands	No	3d Similarity Search Ligands
9	Pinostrobin chalcone	9	Hesperetin chalcone
10	Licoagrochalcone A	10	Homoeriodictyol chalcone
11	Xanthoangelol B	11	Flemichapparin
12	Morachalcone A	12	Flavokawain C
13	Angusticornin B	13	Calythropsin
14	2,2',4'-Trihydroxychalcone	14	Homobutein
15	Isobavachalcone	15	Broussonin B
16	3'-geranylchalconaringenin	16	Anemarchalconyn
17	Bavachalcone	17	Rhusopolyphenol F
18	Xanthoangelol C	18	Lanceoletin
19	Stipulin	19	Bauhiniasin
20	Desmethylxanthohumol	20	Nyasol
21	Kanzonol C	21	Hesperetin dihydrochalcone
22	Bartericin A	22	Echinatin
23	Isocordoin	23	Licochalcone B
24	Abyssinone VI	24	Neoplathymenin
25	Sanjuanolide	25	Kukulkanin B
26	Jejuchalcone B	26	Asebogenin
27	Kuwanol D	27	Heliannone A
28	Sophoradin	28	Xenognosin
29	Ammothamnidin	29	Sappanchalcone
30	Linderachalcone	30	Peltochalcone

Notes: = Overlapping result between 2D and 3D similarity search

Structurally, 2D-derived ligands exhibited high conservation of the benzene ring connected to a three-carbon chain with a carbonyl group adjacent to the ring, supplemented by two hydroxyl groups at the ortho and para positions (Figure 1). Phloretin demonstrated the highest relevance in the 2D search. In contrast, 3D-derived ligands, such as pinochembrine chalcone, showed high atomic arrangement similarity to isoliquiritigenin but displayed distinct conformational variations.

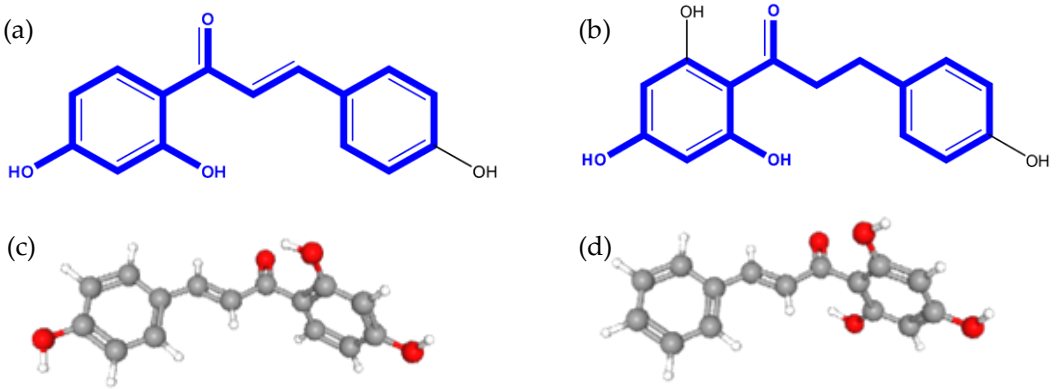


Figure 1. Structural correspondence of lead candidates derived from similarity searches. Top: 2D structural comparison between (a) isoliquiritigenin and (b) phloretin, where blue highlights indicate the conserved scaffold. Bottom: 3D conformational alignment of (c) isoliquiritigenin and (d) pinochembrine chalcone illustrating spatial similarity.

3.2. Molecular Docking Validation

Validation was performed using the FLT3 receptor (PDB ID: 6JQR) co-crystallized with gilteritinib (2.20 Å resolution). Validation of the FLT3 X-ray structure yielded an R_{free} of 0.222 and an RSRZ outlier rate of 2.7%, confirming a strong correlation between the model and experimental data (Figure 2). Stereochemical analysis further demonstrated high structural integrity, with a clashscore of 0 and 0% outliers for both Ramachandran and sidechain geometries.

Redocking of the native ligand (gilteritinib) was conducted across a grid box range of 1.0 to 5.0 Å. A grid box size of 1.0 Å yielded the minimum RMSD of 0.1191 Å, which is well below the 2.0 Å acceptance threshold. The ΔG for the validated pose was -8.435 kcal/mol. Interaction analysis confirmed that the redocked pose maintained contact with key inhibitory residues, including K644, C694, F691, E692, N701, D829, and F830, ensuring the reliability of the docking parameters for subsequent screening.

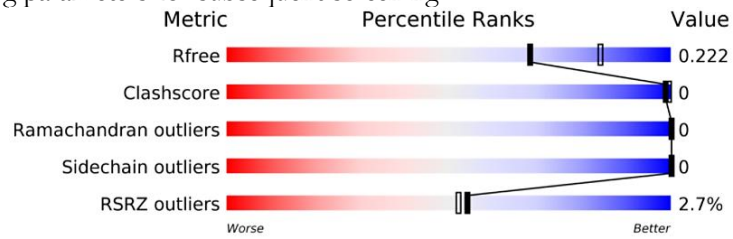


Figure 2. X-ray structure validation of FLT3 crystal (PDB ID: 6JQR)

3.3. Virtual Screening and Interaction Analysis

Virtual screening of 60 candidate ligands was executed in two stages. The first stage identified 32 ligands with binding affinities superior to the control isoliquiritigenin (ΔG < -7.767 kcal/mol). The second stage narrowed the selection to 14 ligands that outperformed the native inhibitor gilteritinib with ΔG < -8.435 kcal/mol (Table 2).

Molecular docking of the 14 lead candidates revealed that sophoradin exhibited the most negative binding energy, indicating the highest inhibitory potential, whereas linderachalcone displayed the least negative affinity among the finalists. Interaction mapping identified hydrogen bonds, hydrophobic contacts, and van der Waals forces as the primary stabilizing factors within the binding pocket. Hydrogen bonding was predominantly observed at residue C694, characterized by bond lengths exceeding 2.8 Å. Hydrophobic interactions were consistently identified at the catalytic residues F691 and K644, mediated primarily through π-alkyl and π-π stacking involving the aromatic rings of the ligands. Additionally, van der Waals forces were dominant at the D829 catalytic residue, frequently involving the saturated carbon chains of the flavonoid scaffolds.

Table 2. Selected lead candidates identified through virtual screening.

Ligand	ΔG(kcal/mol)	K_d (pM)
Gilteritinib (native)	-8,435	6,56 x 10^5
Isoliquiritigenin (control)	-7,767	2,02 x 10^6
Sophoradin	-9,697	7,80 x 10^4
Kanzonol C	-9,359	1,38 x 10^5
Bartericin A	-9,323	1,47 x 10^5
Paratocarpin E	-9,200	2,53 x 10^5
Stipulin	-8,950	2,75 x 10^5
Abyssinone VI	-8,936	2,82 x 10^5
Jejuchalcone B	-8,796	3,57 x 10^5
Kuwanol D	-8,796	3,57 x 10^5
Licoagrochalcone A	-8,788	3,62 x 10^5
Angusticornin B	-8,767	3,75 x 10^5
3'-Geranylchalconaringenin	-8,722	4,04 x 10^5
Bavachalcone	-8,662	4,47 x 10^5
Peltochalcone	-8,491	5,97 x 10^5
Linderachalcone	-8,476	6,12 x 10^5

3.4. Structural Correspondence and Receptor Affinity

The comparative analysis of 2D and 3D similarity search results revealed distinct variations in binding affinities and structural relevance. Ligands identified through 2D similarity search, prioritized by substructure fingerprints, yielded ΔG values ranging from -7.208 to -9.697 kcal/mol, with phloretin and linderachalcone exhibiting the highest and lowest relevance, respectively. Conversely, ligands from the 3D similarity search, sorted by Gaussian-shape functions, showed narrower and higher energy ranges between -6.681 and -

8.491 kcal/mol. In this group, pinocembrine chalcone demonstrated the highest structural similarity, while naringenin chalcone was the least relevant based on 3D shape alignment.

Structural superposition against isoliquiritigenin highlighted that high 2D similarity scores strongly correlated with congruent binding poses. Phloretin showed a near-identical spatial orientation to the reference, whereas linderachalcone displayed a significantly different alignment (Figure 3a-b). In the 3D similarity cohort, naringenin chalcone achieved a more precise superposition than pinocembrine chalcone, despite the latter's higher relevance score, as pinocembrine's aliphatic chain caused a spatial deviation from the reference ligand's scaffold (Figure 3c-d).

The relationship between thermodynamic stability and binding pose indicated that the most negative ΔG did not necessarily guarantee structural mimicry of the reference. Sophoradin, which possessed the most negative ΔG, exhibited a pose that diverged from isoliquiritigenin. In contrast, hesperetin dihydrochalcone, characterized by the most positive ΔG among the selected candidates, maintained a superposition that was highly consistent with the reference ligand (Figure 3e-f). These results suggest that while 2D similarity is a reliable predictor of binding pose, 3D shape similarity and binding energy provide independent vectors for evaluating receptor-ligand interactions.

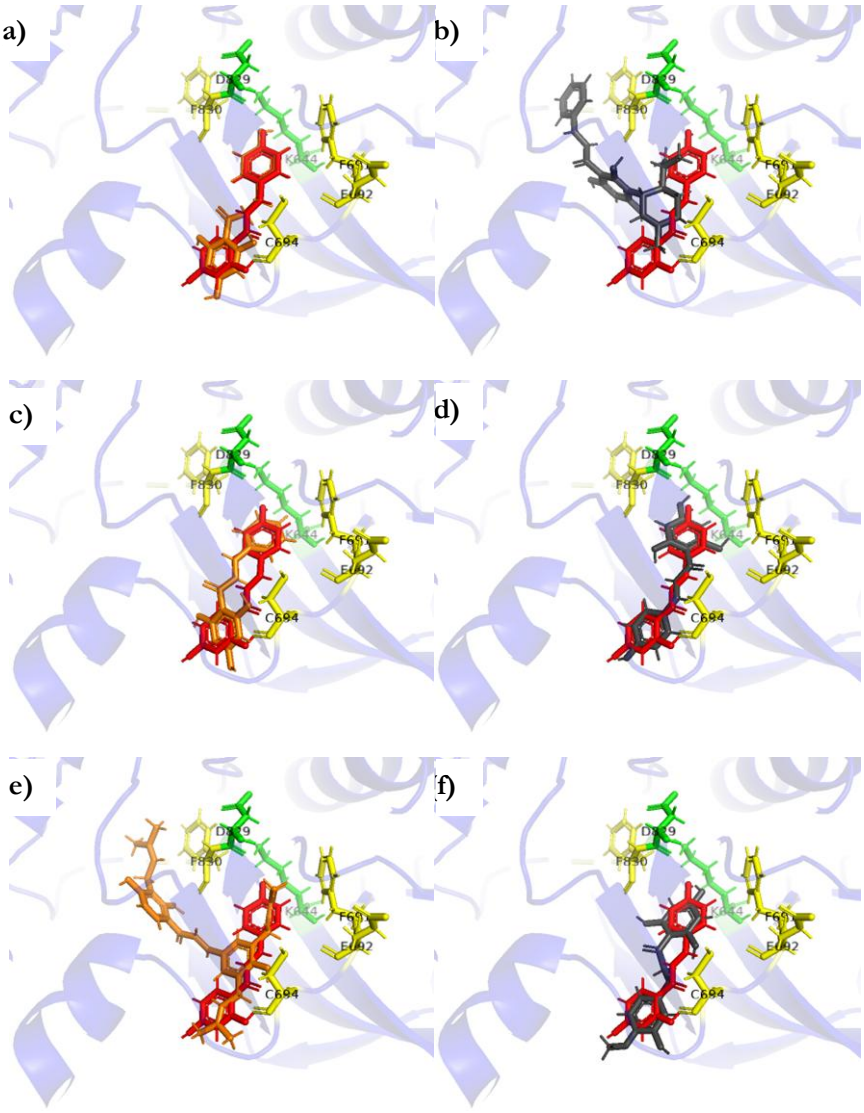


Figure 3. Structural superposition of selected ligands onto the isoliquiritigenin reference pose. (a-b) 2D similarity cohort: phloretin (highest relevance) versus linderachalcone (lowest relevance). (c-d) 3D similarity cohort: naringenin chalcone versus pinocembrine chalcone. (e-

f) Binding-energy extremes among selected candidates: sophoradin (most negative ΔG) versus hesperetin dihydrochalcone (least negative ΔG).

3.5. Bioavailability and Toxicity Prediction

Pharmacokinetic evaluation showed that all 14 lead ligands adhered to the fundamental requirements for bioavailability, although seven compounds (including sophoradin and kuwanol D) exceeded the Lipinski limit for LogP>5 (Table 3). Notably, the native ligand gilteritinib violated three Lipinski rules, whereas the 14 test ligands showed more favorable drug-likeness profiles.

Toxicity screening indicated that all 14 ligands were weak hERG inhibitors and non-carcinogenic (Table 4). Acute oral toxicity assessment categorized peltochalcone as Category II (toxic), leading to its exclusion. Consequently, 13 ligands were identified as viable drug candidates with safe toxicological profiles and high predicted bioavailability.

Table 3. Physicochemical properties and Lipinski's Rule of Five screening

Ligand	Molar Refractivity	Molecular Weight (Da)	H-Bond Donor	H-Bond Acceptor	LogP
Gilteritinib (native)	168,43*	552,71*	3	11*	3,48
Isoliquiritigenin (control)	72,32	256,25	3	4	2,70
Sophoradin	143,48*	460,60	3	4	7,23*
Kanzonol C	119,75	392,48	3	4	5,71*
Bartericin A	120,91	408,48	4	5	4,68
Paratocarpin E	120,91	408,48	4	5	4,68
Stipulin	119,75	392,48	3	4	5,71*
Abyssinone VI	119,75	392,48	3	4	5,71*
Jejuchalcone B	120,79	408,48	4	5	4,90
Kuwanol D	121,62	408,48	4	5	5,64*
Licoagrochalcone A	96,03	324,37	3	4	4,20
Angusticornin B	122,08	424,48	5*	6	3,65
3'-geranylchalconaringenin	121,62	408,48	4	5	5,64*
Bavachalcone	96,03	324,37	3	4	4,20
Peltochalcone	78,27	300,26	4	6	2,26
Linderachalcone	117,95	392,48	3	6	5,79*

Note: Values followed by (*) and indicated in bold exceed the Lipinski Rule of Five thresholds (MW < 500, LogP < 5, HBD < 5, HBA < 10) or Molar Refractivity limits (40–130).

Table 4. In silico toxicological profiling

Ligand	hERG Inhibition	Carcinogenicity	Acute Oral Toxicity
Gilteritinib (native)	(IL) 0,9932	(NK) 0,8554	(III) 0,7024
Isoliquiritigenin (control)	(IL) 0,9388	(NK) 0,8639	(III) 0,7921
Sophoradin	(IL) 0,9039	(NK) 0,8677	(III) 0,7077
Kanzonol C	(IL) 0,9329	(NK) 0,8602	(III) 0,7107
Bartericin A	(IL) 0,9330	(NK) 0,8731	(III) 0,7135
Paratocarpin E	(IL) 0,9330	(NK) 0,8731	(III) 0,7135
Stipulin	(IL) 0,9329	(NK) 0,8602	(III) 0,7107
Abyssinone VI	(IL) 0,9039	(NK) 0,8677	(III) 0,7077
Jejuchalcone B	(IL) 0,9649	(NK) 0,8554	(III) 0,6344
Kuwanol D	(IL) 0,7930	(NK) 0,9044	(III) 0,5839
Licoagrochalcone A	(IL) 0,9377	(NK) 0,8808	(III) 0,7270
Angusticornin B	(IL) 0,9126	(NK) 0,8933	(III) 0,6939
3'-geranylchalconaringenin	(IL) 0,7930	(NK) 0,9044	(III) 0,5839
Bavachalcone	(IL) 0,9377	(NK) 0,8808	(III) 0,7270
Peltochalcone*****	(IL) 0,9530	(NK) 0,9637	(II) 0,3618*****
Linderachalcone	(IL) 0,9449	(NK) 0,8401	(III) 0,6645

Note: WI: Weak Inhibitor; NC: Non-carcinogenic; Category III: Low toxicity/Safe. Asterisk (*****) denotes a violation of the safe toxicity threshold (Category II), indicating potential acute oral toxicity.

4. Discussion

4.1 Ligand Selection via Similarity Search

The identification of drug candidates through similarity searching is predicated on the "similarity-property principle," which posits that structurally related molecules are likely to exhibit similar physicochemical properties and biological activities (Bolton *et al.,* 2011). In this study, the use of isoliquiritigenin as a structural template allowed for the mining of the PubChem database to identify flavonoids with potential FLT3 inhibitory activity (Wang *et al.,* 2021). The 2D similarity search, utilizing an 881-bit substructure fingerprint, yielded 2,385 compounds. By applying a Tanimoto coefficient threshold of ≥ 0.9, we ensured that the selected candidates maintained the core scaffold necessary for receptor binding, specifically the branched benzene ring with essential hydroxyl and carbonyl substitutions (Kim *et al.*, 2016).

In contrast, the 3D similarity search focused on the spatial orientation and conformer volume using the Gaussian-shaped overlay method. While 2D methods focus on chemical connectivity, 3D methods evaluate Shape-Tanimoto (ST) and Color-Tanimoto (CT), which represent steric volume and pharmacophoric features (e.g., hydrogen bond donors/acceptors), respectively. Our results showed that 2D-derived ligands generally possessed more negative binding energies than 3D-derived ones. This suggests that while 3D similarity ensures a close fit to the template's conformation, 2D similarity allows for the exploration of a broader chemical space, potentially identifying bioisosteres with optimized electronic properties for the FLT3 pocket. This observation aligns with Kim *et al.*, (2016), who noted that overlapping 2D and 3D hits usually constitute only 2% of a database, yet these intersections often represent the most robust candidates for further lead optimization.

4.2 Molecular Docking Validation

Before executing virtual screening, the docking protocol must be rigorously validated to ensure that the computational model can accurately replicate experimental binding modes. The selection of the FLT3 receptor (PDB ID: 6JQR) was strategic; with a resolution of 2.2 Å, it provides a significantly more reliable atomic coordinate map than the 3.2 Å resolution structures often used in earlier studies. High-resolution structures minimize the uncertainty in side-chain positioning, which is critical for calculating precise binding affinities.

The validation results yielded a Root Mean Square Deviation (RMSD) of 0.1191 Å for the redocked native ligand (gilteritinib). This value is well below the standard 2.0 Å threshold, indicating that the scoring function and grid box parameters (1.0 Å spacing) are highly accurate. Furthermore, the redocking successfully recovered interactions with key residues such as K644, C694, and D829. As highlighted by Smart *et al.*, (2018), maintaining a low clashscore and high Ramachandran stability during these simulations is essential to ensure that the predicted poses are not only energetically favorable but also stereochemically feasible.

4.3 Virtual Screening and Binding Affinity

The virtual screening process served as a high-throughput filter, using the ΔG as the primary metric for selection. Isoliquiritigenin and the clinical drug gilteritinib served as benchmark cutoffs. Out of the initial library, 14 ligands demonstrated ΔG values more negative than both benchmarks, suggesting a higher thermodynamic stability in the FLT3-ligand complex.

Sophoradin emerged as the most promising lead, exhibiting the highest binding affinity. The correlation observed between ΔG and the dissociation constant (K_d) confirms that these top-tier ligands have a low probability of dissociating from the ATP-binding site. According to the principles described by Aswad *et al.*, (2020), a more negative ΔG indicates a more spontaneous and stable formation of the protein-ligand complex. This stability is vital for kinase inhibitors, as they must compete effectively with endogenous ATP, which is present in millimolar concentrations in the cell, to successfully shut down oncogenic signalling.

4.4 Analysis of Molecular Interactions

The efficacy of FLT3 inhibitors is largely determined by their ability to form specific non-covalent interactions within the ATP-binding pocket. Our analysis revealed that the 14 lead ligands formed robust networks involving K644 and D829. These are classified as

catalytic residues; K644 stabilizes the phosphate groups of ATP, while D829 acts as a proton acceptor. By targeting these specific residues, the flavonoids effectively "block" the catalytic machinery of the enzyme.

The interaction profile was dominated by hydrophobic interactions (π-alkyl and π-π stacks) and hydrogen bonds. While hydrogen bonds provide the specificity required for ligand recognition, the hydrophobic interactions with residues like F691 provide the significant entropic drive necessary for high affinity. Notably, the hydrogen bond lengths for our top candidates were consistently < 2.8 Å. According to Ruslin *et al.*, (2015), such short distances are indicative of strong electrostatic attractions, which correlate directly with increased inhibitory potency. The diversity in binding poses among 2D-searched ligands suggests that variations in the flavonoid B-ring can be leveraged to fill sub-pockets within the receptor that are not occupied by the original template.

4.5 Bioavailability and Toxicity Predication

For a compound to transition from an *in silico* hit to a viable drug, it must possess favorable pharmacokinetic properties (Benet *et al.* 2016; Chen *et al.* 2020). Evaluation against Lipinski's Rule of Five revealed that while the commercial drug gilteritinib violated rules concerning molecular weight and hydrogen bond acceptors, the flavonoid candidates remained largely compliant. This suggests that these flavonoids may have superior oral absorption and membrane permeability compared to some current synthetic inhibitors.

The toxicity profiles obtained via admetSAR further bolster the therapeutic potential of these compounds. The classification of these ligands as non-carcinogenic and weak hERG inhibitors is particularly significant. Strong hERG inhibition is a leading cause of cardiotoxicity (Lamothe *et al.* 2016), a common reason for drug failure in clinical trials. Furthermore, the Acute Oral Toxicity results categorized 13 of the 14 ligands into Category III, indicating a high LD50 range and a broad safety margin for oral consumption (Li *et al.* 2014).

This study concludes that similarity-based virtual screening is an effective strategy for identifying novel FLT3 inhibitors from the flavonoid class. Sophoradin was identified as the lead candidate, surpassing the binding affinity and drug-likeness parameters of the clinical reference, gilteritinib. The results suggest that the chalcone-like scaffold of these flavonoids, combined with specific hydroxyl placements, provides an ideal geometry for ATP-competitive inhibition.

Clinically, these findings suggest that sophoradin and the other top-ranked flavonoids may serve as scaffolds for developing FLT3 inhibitors with a more favorable pharmacokinetic and safety profile than gilteritinib, particularly for AML patients who develop resistance or dose-limiting toxicity with current synthetic inhibitors. Before any translational application, however, these in silico findings must be corroborated experimentally. Future work should prioritize in vitro enzymatic and cell-based FLT3 inhibition assays, co-crystallization or cryo-EM studies to confirm the predicted binding poses, and in vivo pharmacokinetic and toxicity studies in AML models to validate the ADMET predictions reported here.

References

1. Aswad, M., Christine, L., Nursamsiar, & Hardianti, B. (2020). Studi penambatan molekul senyawa-senyawa bioaktif dari kulit akar murbei (Morus sp.) terhadap reseptor TNF-α. Majalah Farmasi dan Farmakologi, 23(3), 85–100.
2. Basilico, S., & Gottgens, B. (2017). Dysregulation of haematopoietic stem cell regulatory programs in acute myeloid leukaemia. Journal of Molecular Medicine, 95(7), 719–727.
3. Benet, L. Z., Hosey, C. M., Ursu, O., & Oprea, T. I. (2016). BDDCS, the rule of 5 and drugability. Advanced Drug Delivery Reviews, 101, 89–98.
4. Birbrair, A., & Frenette, P. S. (2016). Niche heterogeneity in the bone marrow. Annals of the New York Academy of Sciences, 1370(1), 82–96.
5. Bolton, E. E., Chen, J., Kim, S., Han, L., He, S., Shi, W., & Bryant, S. H. (2011). PubChem3D: A new resource for scientists. Journal of Cheminformatics, 3(1), 1–15.
6. Cao, Z. X., Wen, Y., He, J. L., Huang, S. Z., Gao, F., Guo, C. J., & Peng, C. (2019). Isoliquiritigenin, an orally available natural FLT3 inhibitor from licorice, exhibits selective anti–acute myeloid leukemia efficacy in vitro and in vivo. Molecular Pharmacology, 96(5), 589–599.

7. Chen, X., Li, H., Tian, L., Li, Q., Luo, J., & Zhang, Y. (2020). Analysis of the physicochemical properties of acaricides based on Lipinski's rule of five. Journal of Computational Biology, 27(9), 1–10.
8. Choudhary, M. I., Shaikh, M., Tul-Wahab, A., & Ur-Rahman, A. (2020). In silico identification of potential inhibitors of key SARS-CoV-2 3CL hydrolase (Mpro) via molecular docking, MMGBSA predictive binding energy calculations, and molecular dynamics simulation. PLoS One, 15(7), 1–15.
9. Daina, A., Michielin, O., & Zoete, V. (2017). SwissADME: A free web tool to evaluate pharmacokinetics, drug-likeness and medicinal chemistry friendliness of small molecules. Scientific Reports, 7(1), 1–13.
10. Dallakyan, S., & Olson, A. J. (2015). Small-molecule library screening by docking with PyRx. Methods in Molecular Biology, 1263, 243–250.
11. Egbuna, C., Patrick-Iwuanyanwu, K. C., Onyeike, E. N., Khan, J., & Alshehri, B. (2021). FMS-like tyrosine kinase-3 (FLT3) inhibitors with better binding affinity and ADMproperties than sorafenib and gilteritinib against acute myeloid leukemia: In silico studies. Journal of Biomolecular Structure and Dynamics, 1–12.
12. Land, H., & Humble, M. S. (2018). YASARA: A tool to obtain structural guidance in biocatalytic investigations. Methods in Molecular Biology, 1685, 43–67.
13. Jagannathan-Bogdan, M., & Zon, L. I. (2013). Hematopoiesis. Development, 140(12), 2463–2467.
14. Kantarjian, H., Kadia, T., DiNardo, C., Daver, N., Borthakur, G., Jabbour, E., & Ravandi, F. (2021). Acute myeloid leukemia: Current progress and future directions. Blood Cancer Journal, 11(2), 1–25.
15. Kawase, T., Nakazawa, T., Eguchi, T., Tsuzuki, H., Ueno, Y., Amano, Y., Suzuki, T., Mori, M., & Yoshida, T. (2019). Effect of Fms-like tyrosine kinase 3 (FLT3) ligand (FL) on antitumor activity of gilteritinib, a FLT3 inhibitor, in mice xenografted with FL-overexpressing cells. Oncotarget, 10(58), 6111–6123.
16. Kim, S., Thiessen, P. A., Bolton, E. E., Chen, J., Fu, G., Gindulyte, A., & Bryant, S. H. (2016). PubChem substance and compound databases. Nucleic Acids Research, 44(1), 1202–1213.
17. Kopustinskiene, D. M., Jakstas, V., Savickas, A., & Bernatoniene, J. (2020). Flavonoids as anticancer agents. Nutrients, 12(457), 1–25.
18. Lamothe, S. M., Guo, J., Li, W., Yang, T., & Zhang, S. (2016). The human ether-a-go-go-related gene (hERG) potassium channel represents an unusual target for protease-mediated damage. Journal of Biological Chemistry, 291(39), 20387–20401.
19. Li, X., Chen, L., Cheng, F., Wu, Z., Bian, H., Xu C., Li, W., Liu, G., Shen, X., & Tang, Y. (2014). In silico prediction of chemical acute oral toxicity using multi classification methods. Journal of Chemical Information and Modeling, 54(4), 1061–1069.
20. Nombela-Arrieta, C. G., & Manz, M. (2017). Quantification and three dimensional microanatomical organization of the bone marrow. Blood Advances, 1(6), 407–416.
21. Ochieng, P. J., Sumaryada, T., & Okun, D. (2017). Molecular docking and pharmacokinetic of herbal derivatives as maltase-glucoamylase inhibitor. Asian Journal of Pharmaceutical and Clinical Research, 10(9), 392–398.
22. Papaemmanuil, E., Gerstung, M., Bullinger, L., Gaidzik, V. I., Paschka, P., Roberts, N. D., Potter, N. E., Heuser, M., Thol, F., Bolli, N., Gundem, G., Haferlach, C., ... Campbell, P. J. (2016). Genomic classification and prognosis in acute myeloid leukemia. The New England Journal of Medicine, 374(23), 2209–2221.
23. Ruslin, Sutrisna, R., & Arba, M. (2015). Studi penambatan molekul beberapa senyawa turunan imidazolidin sebagai antiinflamasi. Majalah Farmasi, Sains, dan Kesehatan, 1(1), 4–7.
24. Smart, O. S., Horský, V., Gore, S., Svobodová Vařeková, R., Bendová, V., Kleywegt, G. J., & Velankar, S. (2018). Worldwide Protein Data Bank validation information: Usage and trends. Acta Crystallographica Section D: Structural Biology, 74(3), 237–244.
25. Sutamtewagul, G., & Vigil, C. E. (2018). Clinical use of FLT3 inhibitors in acute myeloid leukemia. OncoTargets and Therapy, 11, 7041–7052.
26. Vos, T., Allen, C., Arora, M., Barber, R. M., Bhutta, Z. A., Brown, A., ... Murray, C. J. L. (2016). Global, regional, and national incidence, prevalence, and years lived with disability for 310 diseases and injuries, 1990–2015: A systematic analysis for the Global Burden of Disease Study 2015. The Lancet, 388(10053), 1545–1602.
27. Wang, K. L., Yu, Y. C., & Hsia, S. M. (2021). Perspectives on the role of isoliquiritigenin in cancer. Cancers, 13(115), 1–37.